Cause of the Lower-Hybrid Current-Drive Density Limit

L. H. Sverdrup[a] and P. M. Bellan
California Institute of Technology, Pasadena, California 91125
(Received 13 April 1987)

We derive a simple model which predicts the observed lower-hybrid current-drive density limit for all major experiments to within a factor of 2. The model is based on (i) the experimentally observed upshift in $k_\parallel$ and (ii) the $k_\parallel$ dependence of the mode coalescence condition of the linear model conversion of a lower-hybrid wave into a hot-plasma wave.

PACS numbers: 52.40.Db, 52.25.Sw, 52.50.Gj, 52.55.Fa

Fisch[1] predicted in 1978 that dc toroidal currents could be driven in tokamaks by the injection of suitably phased lower-hybrid waves. Prior to 1978, lower-hybrid experiments had been designed to provide ion heating via the linear mode conversion process predicted by Stix[2] to occur at the lower-hybrid layer where $\omega=\omega_{lh}$. Initial attempts to reconfigure these heating experiments so as to produce current drive were unsuccessful, until Yamamoto *et al.*[3] demonstrated on the JFT-2 tokamak that current could be driven provided that the plasma density was reduced substantially from the values typically used in the heating experiments (i.e., the density was reduced so that $\omega>2\omega_{lh}$). The JFT-2 results have been subsequently reproduced and extended in a large number of devices,[4-18] and it has always been found that current drive works only up to a (rather low) "density limit" where mode conversion would not be expected since $\omega>2\omega_{lh}$. Experiments indicate that the density limit increases with[16] ω and[13] m_i. The density limit is not predicted in Fisch's theory. Tonon and Moulin,[19] and Wegrowe and Engelmann[20] postulated a density-limit mechanism based on the wave interacting with hot ions, but (as we will show) their model predicts the density limit to have a strong singularity, inconsistent with experimental observations.

We present here a new and very simple model which predicts within a factor of 2 the observed density limits of all major current-drive experiments. This model is based upon (i) the dependence on parallel wave number $k_\parallel$ of the coalescence of the two modes involved in linear mode conversion of a lower-hybrid wave into a hot-plasma wave and (ii) the upshift in $k_\parallel$ that is associated with the filling of the spectral gap in current drive. Before deriving the model, let us briefly review (i) and (ii).

$k_\parallel$ dependence of mode coalescence.—Stix[2] showed that when hot-plasma effects are included, the lower-hybrid dispersion relation becomes

$$k_\perp^4\epsilon_{th}+k_\perp^2\epsilon_\perp+k_\parallel^2\epsilon_\parallel=0, \tag{1}$$

where

$$\epsilon_\perp=1-\frac{\omega_{pi}^2}{\omega^2}+\frac{\omega_{pe}^2}{\omega_{ce}^2},\quad \epsilon_\parallel=1-\frac{\omega_{pe}^2}{\omega^2},\quad \epsilon_{th}=-\left(\frac{3}{4}\frac{\omega_{pe}^2}{\omega_{ce}^2}\frac{u\bar{T}_e^2}{\omega_{ce}^2}+3\frac{\omega_{pi}^2}{\omega^2}\frac{u\bar{T}_i^2}{\omega^2}\right). \tag{2}$$

Equation (1) is quadratic in $k_\perp$ giving two modes,

$$k_\perp^2=[-\epsilon_\perp\pm(\epsilon_\perp^2-4k_\parallel^2\epsilon_\parallel\epsilon_{th})^{1/2}]/2\epsilon_{th}, \tag{3}$$

which are plotted in Fig. 1. The small-$k_\perp$ mode is the launched lower-hybrid wave (cold mode) which propagates from the plasma periphery towards the lower-hybrid layer (where $\epsilon_\perp=0$); in the vicinity of this layer the cold mode converts[2] linearly to the large-$k_\perp$ hot-plasma mode which propagates back towards the periphery and is strongly damped. It was originally assumed[2] that mode conversion occurred at the lower-hybrid layer where $\epsilon_\perp=0$ (or equivalently $\omega=\omega_{lh}$), but it was later noted[21,22] that the mode conversion actually occurs at the point where the two modes described by Eq. (3) coalesce, i.e., where

$$k_\parallel=\epsilon_\perp^2/4\epsilon_{th}\epsilon_\parallel. \tag{4}$$

Examination of Fig. 1 shows that the location of mode coalescence is at a lower density than the lower-hybrid layer, and Eq. (4) shows that this location depends on a large number of parameters.

Upshift of $k_\parallel$.—There is a well-known[23,24] problem

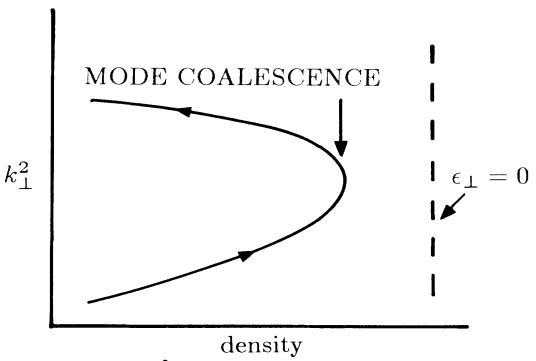

FIG. 1. Plot of $k_\perp^2$ vs density. Note that the location of mode coalescence occurs at lower density (Ref. 21) than the location of the lower-hybrid layer.

concerning the use of Fisch's theory to explain the results of current-drive experiments. According to Fisch's theory, lower-hybrid waves drive current by imparting momentum to electrons in the tail of the distribution function. These electrons can interact with the wave because their velocity u satisfies the resonance condition $u=\omega/k_\parallel$. Yet, in all experiments[14] the parallel refractive index launched is typically $n_\parallel=ck_\parallel/\omega=1.5$–$10$ so that, in order for electrons to be resonant with the wave, they must have $3\times10^9<u<2\times10^{10}$. In the experiments the electron temperature has ranged from 50 to 2000 eV ($3\times10^8<u_{T_e}<1.3\times10^9$). Thus, except for the hottest of these plasmas, there ought to be essentially zero electrons capable of resonantly interacting with the wave. What seems to happen is that the wave creates its own tail by pulling electrons from the bulk out to high velocities via parallel-wave–partial resonant interaction. In order to do this, at least some component of the launched wave $k_\parallel$ spectrum must interact resonantly with electrons in the bulk, and so a spectral component must develop which has a parallel phase velocity much lower than the launched value. In effect, $k_\parallel$ has been shifted up for some fraction of the launched wave power (the remainder is, of course, unshifted and interacts with the newly created tail electrons to give current drive as predicted by Fisch). Various mechanisms for the upshift have been proposed, such as toroidal-poloidal[22] and ponderomotive[24] effects. It has also been suggested[23] that there is no upshift, but that the antenna spectrum includes enough of a large-$k_\parallel$ component to pull electrons from the bulk to high velocities.

We will not attempt here to decide which (if any) of the above mechanisms cause the $k_\parallel$ upshift. Instead, we will simply accept the upshift as an experimentally observed fact; i.e., experiment has shown that $k_\parallel$ is shifted up for part of the launched power in such a way that

$$k_\parallel=\omega/\gamma u_{T_e}, \tag{5}$$

where $\gamma\approx1$–2.

We postulate that the density limit occurs when the $k_\parallel$ predicted by Eq. (5)—i.e., the $k_\parallel$ interacting with the bulk—is of such a value to satisfy Eq. (4). When this occurs, (i) mode conversion takes place for the upshifted $k_\parallel$ component which thus becomes strongly attenuated by *perpendicular*[2] damping processes, and so cannot pull electrons from the bulk to the tail by *parallel*-wave–particle resonance, so that (ii) there are no tail electrons to resonantly interact with the unshifted (i.e., high phase velocity) component of the incoming wave, and so (iii) there is no current drive. We emphasize that, for the upshifted $k_\parallel$ component, mode conversion takes place even though $\omega>\omega_{\rm lh}$.

Proceeding with the mathematical derivation, we define $x=\omega_{pe}^2/\omega^2$, so that $\epsilon_\parallel=-x$, $\epsilon_\perp=1-\lambda x$, where $\lambda=m_e/m_i-\omega^2/\omega_{ce}^2$, and $\epsilon_{\rm th}=-x\alpha u_{T_e}^2/\omega^2$ where $\alpha=\frac{3}{4}\beta_e\omega^4/\omega_{ce}^4+3(m_e/m_i)^2\beta_iT_i/T_e$. (Here, we have introduced the temperature enhancement factors β_e,β_i which multiply the bulk temperatures T_e,T_i. These enhancement factors take into account the fact that the total energy in rf-produced suprathermal tails can, depending on rf power levels, be comparable to the energy of the bulk; in particular, β_e will exceed unity when the fast electrons providing current drive have a total energy comparable to the bulk,[5] while β_i will exceed unity when there is ion heating.[20]) Using Eq. (5) in Eq. (4), we find $x=1/(2\alpha^{1/2}+\lambda)$, or in terms of the original variables

$$\frac{\omega_{pe}^2}{\omega^2}=\left[\frac{2}{\gamma}\left(\frac{3}{4}\beta_e\frac{\omega^4}{\omega_{ce}^4}+3\beta_i\frac{m_e^2}{m_i^2}\frac{T_i}{T_e}\right)^{1/2}+\frac{m_e}{m_i}-\frac{\omega^2}{\omega_{ce}^2}\right]^{-1}. \tag{6}$$

All the major current-drive experiments had $T_i/T_e\simeq0.3-1$; however, there was a fairly large range of frequencies, magnetic fields, and observed density limits. Figure 2 plots Eq. (6) for hydrogen (solid lines) and for deuterium (dashed lines) and also shows the experimentally measured normalized density limits of a large number of experiments. Here we have chosen $\gamma=\beta_e=\beta_i=1$ as plausible values which give a good fit to the observations [note, that according to Eq. (6), equally plausible values of $\gamma=1.4$, $\beta_e=\beta_i=2$ would give the same results]. Figure 2 also plots Eq. (6) for argon which was used in the Caltech Encore plasma.[25] Table I presents the same information but with nonnormalized parameters; hydrogen gas is assumed, unless specified otherwise, and for case where T_i and/or T_e were unspecified, an estimate of $T_i/T_e=0.3$ was used to calculate the predicted density limit.

It is clear from Fig. 2 and Table I that Eq. (6) predicts the experimental observations for a wide variety of parameters. Several[8,13,16] experiments were carefully controlled so as to determine the dependence on just one parameter. Equation (6) is consistent with the observations of these experiments: in particular, Eq. (6) is consistent with the dependence on ω observed in Versator[16] and Petula-B,[11,18] the dependence on B observed in FT,[8] and the dependence on m_i observed in ASDEX.[13]

From Eq. (6) and Fig. 2 it is seen that there are essentially two regimes of interest: (i) a low-field region (slope on left-hand side of Fig. 2) where the density limit is independent of ω and proportional to B^2, and (ii) a high-field region (flat portion of curve in Fig. 2) where the density limit is independent of B and is instead determined by T_i/T_e, ω, and m_i. The change from regime (i) to regime (ii) occurs at $\omega\approx\omega_{\rm gm}(2T_i/T_e)^{1/2}$, where $\omega_{\rm gm}=(\omega_{ci}\omega_{ce})^{1/2}$ is the geometric mean frequency.

It is worthwhile to compare our model to that proposed by Wegrowe and Engelmann[20] (the Tonon and

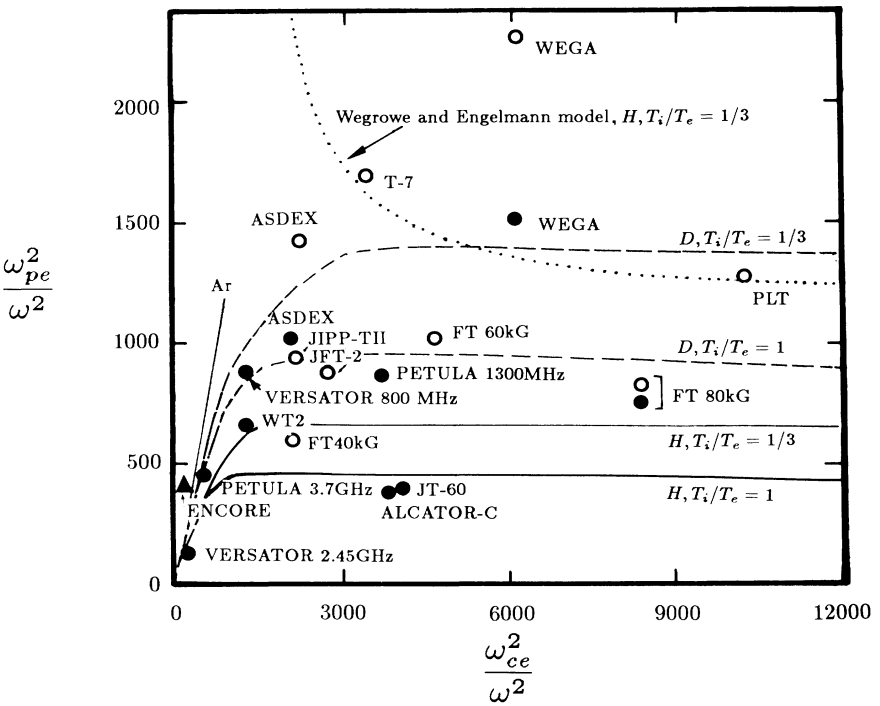

FIG. 2. Density limit predicted by Eq. (6) vs experiments: The solid line is Eq. (6) for hydrogen and the dashed line is for deuterium. For experiments, solid circles indicate hydrogen, open circles indicate deuterium, and the triangle indicates argon (all references in Table I). For comparison, the dotted line shows the Wegrowe and Engelmann model (Ref. 20) [Eq. (7) in text] for hydrogen, $T_i/T_e = \frac{1}{3}$.

TABLE I. Comparison of observed density limit with prediction of Eq. (6).

	f (MHz)	B (kG)	T_i (eV)	T_e (eV)	n_{observed} (10^{12} cm^{-3})	$n_{\text{Eq. (6)}}$ (10^{12} cm^{-3})
JFT-2 (D gas)[a,b]	750	14		250	6	9
Versator[c]	800	10	120	350	7	5
Versator[c]	2450	10	120	350	10	12
PLT (D gas)[d,b]	800	30			10	11
WT-2[e,b]	915	11	50	200	7	7
Alcator-C[f]	4600	100			100	180
FT (D gas)[g,h,i]	2450	40			45	94
FT (D gas)[g,h,i]	2450	60			75	103
FT (D gas)[g,h,i]	2450	80			60	100
FT[g,h,i]	2450	80			55	48
WEGA[i]	800	22.5			12	5
WEGA (D gas)[i]	800	22.5			18	11
T7(D gas)[j]	900	19			17	14
Petula-B[k]	1300	28		1000	18	14
Petula-B[l]	3700	28		1000	80	73
JIPP-TII[m,f]	750	14			8	6
ASDEX[n]	1300	22			20	15
ASDEX (D gas)[n]	1300	22			30	27
JT-60[o]	2000	45			20	34
Encore (Ar gas)[p]	450	1.5	5	10	1	0.3

[a]Reference 3.
[b]Reference 14.
[c]Reference 16.
[d]Reference 5.
[e]Reference 6.
[f]Reference 15.
[g]Reference 8.
[h]Reference 9.
[i]Reference 20.
[j]Reference 10.
[k]Reference 11.
[l]Reference 18.
[m]Reference 12.
[n]Reference 13.
[o]Reference 17.
[p]Reference 25.

Moulin model[19] is essentially the same as the one in Ref. 20). We consider the standard case where there is one ion species and $Z=1$. Expressing Eq. (12a) of Ref. 20 in our notation gives the Wegrowe and Engelmann density limit as

$$\frac{\omega_{pe}^2}{\omega^2}=\left(\frac{\phi^2}{z_0^2}\frac{m_e}{m_i}\frac{T_i}{T_e}+\frac{m_e}{m_i}-\frac{\omega^2}{\omega_{ce}^2}\right)^{-1}, \tag{7}$$

where ϕ^2/z_0^2 is an adjustable parameter,[20] the value of which is given in Ref. 20 to be $\phi^2/z_0^2=2$. It is easily seen that the right-hand side of Eq. (7) becomes singular when $T_i/T_e=(\omega^2/\omega_{gm}^2-1)/2$; this singular behavior is also shown in Fig. 2, where Eq. (7) has been plotted as a dotted line for the typical case of hydrogen, $T_i/T_e=\frac{1}{3}$.

Finally, let us consider the predictions of our model for typical fusion-reactor parameters. With $T_e=T_i$, average atomic mass ≈ 2.5, $f=8$ GHz, and $\gamma=\beta_e=\beta_i=1$, Eq. (6) gives density limits of 4×10^{14} cm^{-3} for $B=6$ T, and 8×10^{14} cm^{-3} for $B=10$ T.

In summary, we have described how the combination of (i) the experimentally observed upshift of $k_\parallel$ to $k_\parallel=\omega/\gamma u_{T_e}$ and (ii) the $k_\parallel$ dependence of linear mode conversion (of lower-hybrid waves into hot-plasma modes) accounts for the lower-hybrid current-drive limit.

This work was supported by National Science Foundation Grant No. ECS-8414541.

---

[a]Present address: Western Research Corporation, San Diego, CA 92121.

[1]N. J. Fisch, Phys. Rev. Lett. **41**, 873 (1978).

[2]T. H. Stix, Phys. Rev. Lett. **15**, 878 (1965).

[3]T. Yamamoto *et al.*, Phys. Rev. Lett. **45**, 716 (1980).

[4]S. C. Luckhardt *et al.*, Phys. Rev. Lett. **48**, 152 (1982).

[5]S. Bernabei *et al.*, Phys. Rev. Lett. **49**, 1255 (1982).

[6]M. Nakamura *et al.*, J. Phys. Soc. Jpn. **51**, 3696 (1982); S. Tanaka *et al.*, in *Proceedings of the Tenth International Conference on Plasma Physics and Controlled Nuclear Fusion Research, London, 1984* (International Atomic Energy Agency, Vienna, 1985), Vol. 1, p. 623.

[7]M. Porkolab *et al.*, in *Proceedings of the Tenth International Conference on Plasma Physics and Controlled Nuclear Fusion Research, London, 1984* (International Atomic Energy Agency, Vienna, 1985), Vol. 1, p. 463.

[8]A. Santini, in Proceedings of the IAEA Technical Committee Meeting on Non-Inductive Current Drive in Tokamaks, Abington, Oxon, England, 1983, Culham Laboratory Report No. CLM-CD, 1983 (unpublished), p. 278; see also Table I in J.-G. Wegrowe and F. Engelmann, Comments Plasma Phys. Controlled Fusion **8**, 211 (1984).

[9]F. Alladio *et al.*, Nucl. Fusion **24**, 725 (1984).

[10]V. V. Alikkaev *et al.*, in Proceedings of the IAEA Technical Committee Meeting on Non-Inductive Current Drive in Tokamaks, Abington, Oxon, England, 1983, Culham Laboratory Report No. CLM-CD, 1983 (unpublished).

[11]C. Gormezano *et al.*, in Ref. 7, p. 503.

[12]K. Toi *et al.*, in Ref. 7, p. 523.

[13]L. Leuterer *et al.*, in Ref. 7, p. 597.

[14]M. Porkolab, IEEE Trans. Plasma Sci. **PS-12**, 107 (1984).

[15]M. Porkolab *et al.*, Phys. Rev. Lett. **53**, 450 (1984).

[16]M. J. Mayberry *et al.*, Phys. Rev. Lett. **55**, 829 (1985).

[17]M. Yoshikawa *et al.*, in Proceedings of the Eleventh International Conference on Plasma Physics and Controlled Nuclear Fusion Research, Kyoto, Japan, 1986 (to be published), paper A-I-1.

[18]F. Parlange *et al.*, in Ref. 7, p. 557.

[19]G. Tonon and D. Moulin, in Ref. 7, p. 557.

[20]Wegrowe and Engelmann, Ref. 8.

[21]V. Krapchev and A. Bers, Phys. Fluids **21**, 2123 (1978).

[22]P. Bonoli, IEEE Trans. Plasma Sci. **PS-12**, 95 (1984).

[23]S. Succi *et al.*, in Ref. 7, p. 549.

[24]E. Canobbio and R. Croci, in Ref. 7, p. 567.

[25]L. H. Sverdrup and P. M. Bellan, Bull. Am. Phys. Soc. **31**, 1578 (1986).